Numerical Modeling and Analysis of the Tehran-Shahriar Plain Subsidence Using COMSOL Software

1.Seyed Hamidreza Hosseini

PhD Candidate, Department of Civil Engineering,

Engineering and Management of Water Resources, Shahr-e-Qods Branch, Islamic Azad

University, Tehran, Iran.

Email: seyed.hr.hosseini@gmail.com

2-Seyed Habib Musavi-Jahromi

Professor, Department of Civil Engineering, Shahr-e-Qods

Branch, Islamic Azad University, Tehran, Iran.

Email: h-mousavi@srbiau.ac.ir

3- Hossein Mohammadvali Samani

Professor, Department of Civil Engineering, Shahr-e-

Qods Branch, Islamic Azad University, Tehran, Iran.

Email: Hossein.samani@yahoo.com

Abstract

The uncontrolled withdrawal of groundwater resources causes a drop of water levels and increases stress to soil particles which would culminate in the land to subside. The critical plain of Shahriar has, over the last years, been affected by the phenomenon of subsidence. Presence of vital channels, as well as economic, pilgrimage and military sites have turned it into a strategic region which increases the detrimental consequences from the subsidence. This study introduces a novel method to predict and analyze subsidence, known as poroelasticity module of COMSOL software that utilizes the concurrent resolution of equations of fluid motion in a porous medium and mechanical deformation. The numerical model's outputs from 2003 to 2019 in 24 points were compared and verified with levelling surveys and Sentinel 1 radar interferometric images (R^2=0.97), indicating an acceptable correlation between values, good match between interferometric images and zoning subsidence maps derived from software and tendency of the values of root mean square error (RMSEA) and efficiency coefficient toward 0 and 1. The finite element modelling (FEM) output suggested that the mean rate of subsidence will have increased at a slower rate by 13.19 cm by 2031 due to subsequent compaction of upper layers of the aquifer, and by 18.38 cm in points where the thickness of clay and silt layers increases. The study finds that the region

under study has a multi-layer aquifer system, which the clay thickness is thought to be a major factor that affects the subsidence variations and patterns. An increase in the thickness, together with high rates of water pumping and the number of geological units are among the major factors contributing to subsidence.

Keywords: subsidence, Shahriar plain, COMSOL, Aquifer level changes

Tob Regul Sci. ™ 2022;8(2): 434-455
DOI: doi.org/10.18001/TRS.8.2.27

1. Introduction

Subsidence denotes the vertical movement [1], or gradual sudden sinking of the earth's surface [35], caused by various factors of geological dissolution, melting of ice and density of deposits, earth's crust movements and outflow of the lava from the solid earth crus or human activities such as mining [31], uncontrolled abstraction of groundwater and oil drillin [9]. This phenomenon causes such problems as unidentical changes to the height and slope of rivers and waterways as well as water transmission structures, breakage or protrusion of wall casing, sand production and destruction of facilities [12].

One of the most important mechanisms caused by this phenomenon is the sinking of the water table levels [17]. Thus, consequent and seasonal droughts or excessive removal of groundwater aquifers causes the sinking of the water table and subsidence [24].

The ground behavior against the plunging water table level (hydraulic head) can be highly complicated, with its behavioral modelling requiring accurate mathematical and numerical methods. In sum, if the rate of water withdrawal is high, but ground level displacement is low, the ground behavior can be assumed to be elastic from a geo-mechanical view; in other words, deformations are reversible [15]. However, if the displacement is high, the ground behavior has no elastic behavior and the deformations are not fully reversible [32]. Using the Biot Poroelasticity Theory, reversibility of the deformation is calculated from combining the physics of the fluid motion in a porous medium and module of solid mechanics [2].

Today, the notorious phenomenon of subsidence is becoming a global crisis [14], which is unfolding in arid and semi-arid regions [13]. Heigio estimates that 200 major cities across the world are now grappling with this crisis [19 and 7]. This phenomenon has been reported in many countries including Mexico, Australia, Colombia, China, U.S., Thailand, India, Japan, Italy, the Netherlands, Venezuela, Egypt, Saudi Arabia, England, France, Poland, Sweden and Iran [20].

Studies by the UNESCO Working Group on Land Subsidence and some researchers on 42 regions in 15 countries facing subsidence revealed that excessive water withdrawal has been a key factor in all cases of subsidence across the world [25, 26 and 27].

Included in the studies on subsidence is the one by Sharifi Kia (2011) which examined this phenomenon in the Nogh-Bahreman plain via an in vitro-survey method. This time-series study used software to examine the radar data of two European and Japanese satellites, and evaluated the derived findings by field and survey computations. To examine the causes of the subsidence, surface and subsurface geology, land use, hydrology and hydro-geology were analyzed. The research found that for every 2.3. m of groundwater drops in the area under study, 1 cm of subsidence was noted, which, considering the variations of the subsidence scope, water abstraction was regarded to be a positive factor, and precipitation as an improving one [22, 23 and 33].

Also, Nadiri et. al. (2018) used a genetic algorithm to provide a framework to estimate aquifer's subsidence potential. In their study, seven hydrological and geological factors affecting the subsidence, including groundwater drop, aquifer environment, feeding, pumping, land use, aquifer thickness, distance from the fault under study, etc. were examined and the map of plain vulnerability against subsidence was derived [28 and 29].

In 2020, Janbaz et al. used the radar interferometry method to investigate the land subsidence caused by groundwater table level changes, concluding that the average subsidence rate from 2003 to 2017 in the Ghazvin's aquifer was 39.9 mm, and little lower around 33 mm in the entire Ghazvin province. Studies have suggested that the maximum subsidence occurred in areas of the aquifer where the fine-grain layer had greater thickness than other areas. Also, the maximum subsidence rates pertained to Bouin Zahra and areas bordering Takestan where water is most withdrawn from groundwater resources. Finally, the findings noted a correlation between water table drop and thickness of fine-grained layer with regards to the subsidence rate in the Ghazvin province [21].

Rajabi et al. (2021) modelled the subsidence of the Izeh plain using MODFLOW mathematical code. According to this study, the yearly precipitation of the area had dropped by 7.2, 18.71 and 23.7% in later periods under various scenarios, thus reducing the surface feeding of the aquifer. The outcome suggests that the mathematical model used to simulate the Izeh aquifer had an error rate of 16%. A survey of the ground structure changes also showed that the aquifer level will subside by a maximum 1.5 m and minimum 0.9 m in the long term of 20 years [30].

Chao et al. (2021) used a numerical method in a multi-layer aquifer system to investigate the land subsidence caused by groundwater table, concluding that the maximum subsidence caused by a drop of the water table level first occurred in the upper layer of the aquifer, with the subsidence transferring to upper ground layers at an alternative rate, taking into account the hydraulic connection between the layers [16].

Also, Yu et al. (2021) used a numerical model to suggest that groundwater withdrawal since 1984 had caused severe land subsidence in the city of Ningbo, China. The rate of land subsidence, however, decreased as harvesting of groundwater wells was prohibited. In the meantime, regions

close to the extracted wells had experienced lower subsidence due to fast recovery of the groundwater levels, compared to farther regions where wells were being extracted [39].

Duke et al. (2022) conducted a three-dimensional simulation of subsidence in a heterogenous aquifer system in Hui, Taiwan, demonstrating that the distribution of hydro-geological material greatly contributed to the groundwater flow and land subsidence [10].

Due to its proximity to the Iranian capital, the Tehran-Shahriar plain is strategically important and is active in terms of industry and agriculture. The presence of infrastructure such as 200 km main roads and inter-city highways, 120 km railway and 25 km subway lines, 2300 km intra and inter-city routes and passageways, international airports, oil refineries and 30 km oil transfer lines, 70 km high voltage power transmission lines and more than 200 km main gas lines, as well as religious and historical sites such as Shah Abdulazim and Imam Khomeini shrines have added to the significance of this critical plain.

Subsidence began to leave its negative impacts on the plain since 1990, following uncontrolled utilization of groundwater resources. This phenomenon receives less attention for its gradual and incremental process; however, it can cause negative social and economic impacts on the plain [11].

To predict the subsidence process and quantify it, various methods have been offered, the best of which is the numerical method [27 and 28]. This method is capable of simulating the subsidence in a single- and multi-physical form (coupling of two or several physics) []. One of the numerical software is the COMSOL software which has different modules for modeling various multi-physical phenomena. Specifically, the flow subsurface module, together with the solid mechanics module, known as poroelasticity flow in subsidence modeling, can be used. Poroelasticity can be used for the fluid flow and deformations created in the porous medium. Thus, porous medium modelling in COMSOL software requires coupling of two laws; The first law is Darcy's law, which expresses the fluid motion in a porous medium, while the second law is the displacement and deformation of the soil skeleton [6]. The use of these two laws in this study constitutes a new process in the 3-dimensional simulation of subsidence.

2. Area Under Study

The Tehran-Shahriar plain is located in the Tehran province. This plain (Figure 1 in blue) covers a selected part of the entire alluvial zone extending from the eastern Tehran's plain to the Karaj River boundaries, which has an area of 1720 square kilometers. The area under study is the central part of the plain, specified in red in the figure. With an area of 359.6 square kilometers, this plain is located between longitudes 39° 52′ E, and latitude 53° 50′ to 50°, 50′ N.

The mean annual precipitation of the plain stands at 200 mm, while the mean annual evaporation is around 2500 mm [37]. Considering the monthly withdrawal basis of 135 piezometric of observation wells since 1993 to 2019, the groundwater levels are illustrated by a hydrograph diagram in Figure 3 [36].

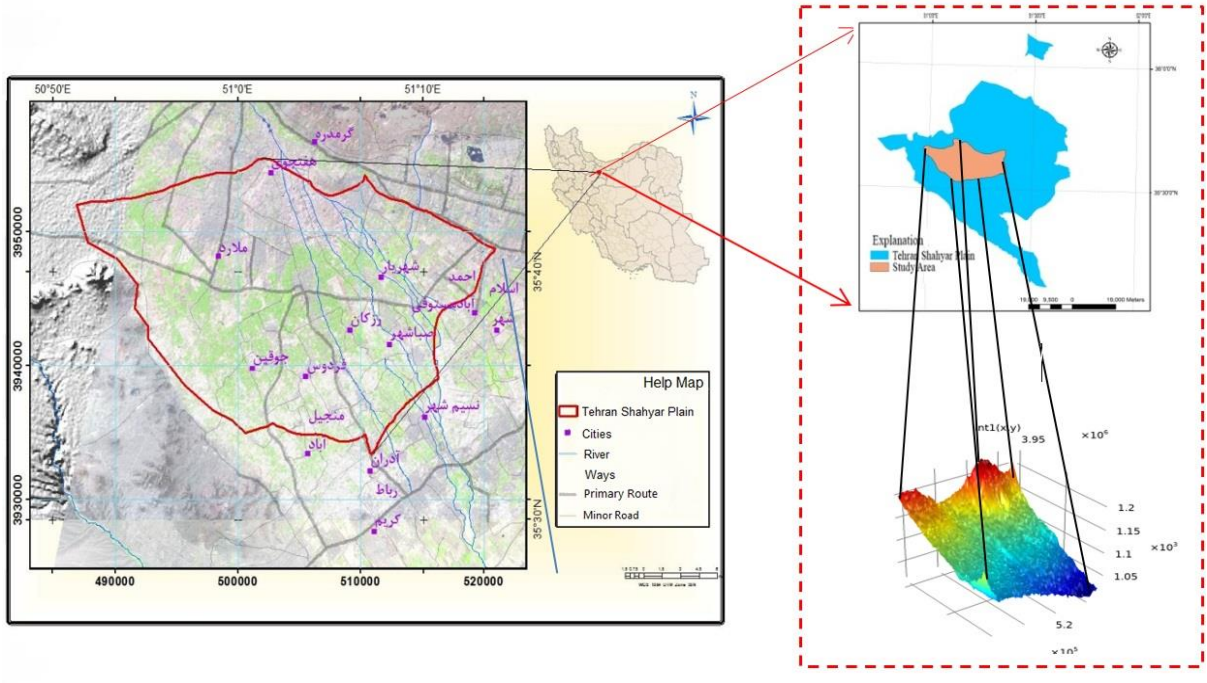

Figure 1- View of Tehran-Shahriar plain and the study area

According to the Ministry of Energy's latest nationwide inventory of water resources in 2020, and consistent with Figure 2, the total number of water wells utilized in the studied area is 3682 rings with an annular discharge rate of around 168.32 million m^3, a major part of which is used in agriculture [36].

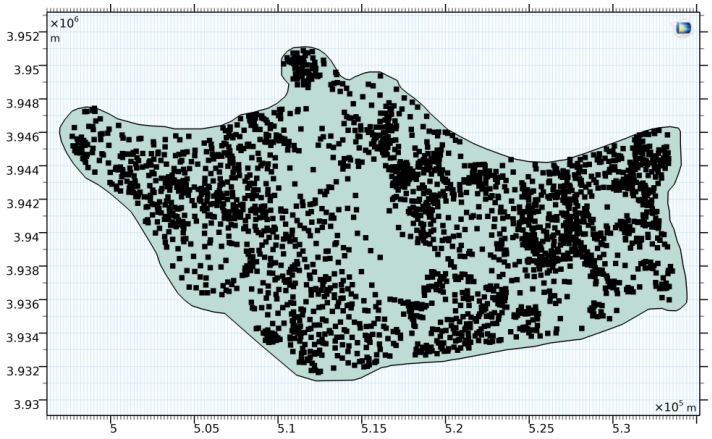

Figure 2 - Spatial distribution of extracted wells in the area under study

Consistent with Figure 3, the mean groundwater level of the sea levels from 1993 to 2019 saw a downtrend of 54 cm each year. The annual water shortage of the aquifer in the area under study in the last five years amounted to around 22 million cubic meters [36].

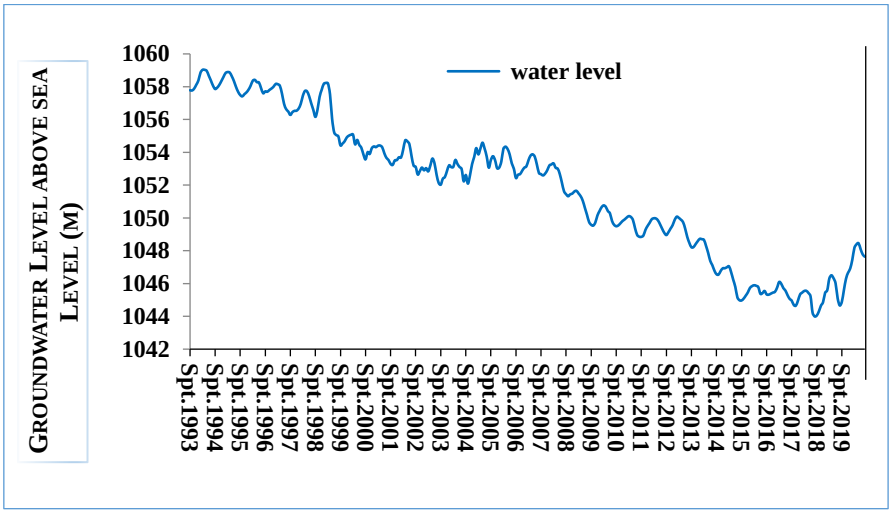

Figure 3- Hydrograph of groundwater unit in Tehran-Shahriar plain, 1993-2019

The area under study lies at the southern foothills of the Central Alborz Mountains and is considered the northernmost subsidence of Central Iran. The northern and southern areas under study constitute Alborz's building unit and Central Iran's building, respectively, located between the Kan and Karaj Rivers. The topography of this area is even. The maximum height difference reaches 35 m. The plain's surface involves young alluvial fans, unconsolidated loose-cement flood, and river deposits of around 60 m thick. Three segments can be noted in the alluvia of this series. Its upper part is made of clay and red soil; its middle part includes round cobblestones and its bottom parts are made of gravels with some clay. In other words, the major part of the plain is made of fine-grained sediments with high storage capacity and some coarse-grained sediments with high permeability [29].

The geological characteristics of the area under study are given in Figure 4 [8].

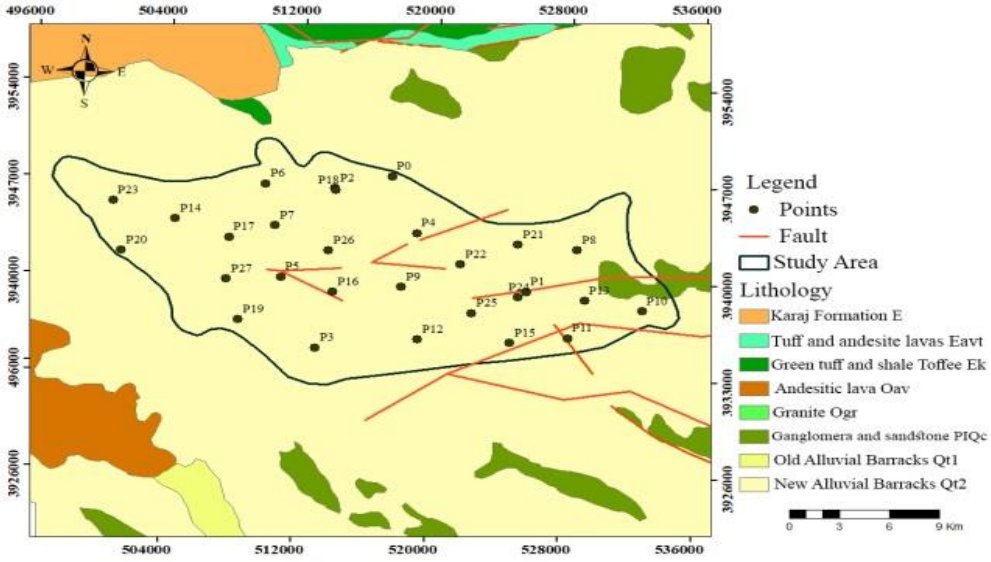

Figure 4- Geological characteristic and faults map in model

3. Research Method

3.1. Modelling subsidence

Land subsidence was developed by Biot in 1941 which was built on the theory of poroelasticity. This theory indicates the elastic behavior of porous material when the fluid between particle spaces is reduced [2]. Modelling the phenomenon of subsidence using the concept of effective stress was first proposed by Terzaghi in 1925. Excessive withdrawal of groundwater can reduce pore pressure and increase effective stress. The increases in effective stress can cause ground layers to compact. Layers of the ground which have low permeability and are composed of more clay and silt have greater levels of compressibility and consolidation than in areas where the layers are composed of sand grains [34]. As the effective stress is greater than the maximum effective stress applied to the soil, soil particles change their arrangement in order to stand against this over-stress, thus reducing reversibility of the volume of soil voids, known as inelastic soil compressibility [10 and 18].

3.2. Governing Equations

The Biot's mathematical model is used for a saturated medium and modeling subsidence caused by groundwater abstraction of the aquifer. This theory is used to calculate the pore-water pressure and soil skeleton deformation.

To use this theory, the following hypotheses should be considered:

1. The Terzaghi's principle of effective stress between the granules must be met on the scale of granules composing soil
2. Soil skeleton deformation occurs due to changing of the soil voids, with soil granules considered as incompressible.

3.2.1. Mathematical Equation Governing on the Problem

This section briefly concerns the mathematical theories and equations governing the numerical modelling of subsidence [2,3,4 and 38]. Consistent with the Terzaghi's theory, effective stress between soil particles is calculated from Equation (1):

$$\sigma' = \sigma - p \quad (1)$$

Where p represents pore-water pressure, and σ' is the effective stress. The pore pressure p, defined according to Equation (2), has p_e representing the increasing pressure and p_s representing static behavior.

$$p = p_s + p_e = (H - \text{Ele})\gamma_w \quad (2)$$

Also, H is the total head and Ele is the height head, while γ_w is the unit specific weight of water. Assuming the problem is three-dimensional in accordance with Figure 5, the mathematical equation (1) can be written in the form of a matrix as in Equation (3):

$$\begin{Bmatrix} \sigma'_x \\ \sigma'_y \\ \sigma'_z \\ \tau'_{XY} \\ \tau'_{XZ} \\ \tau'_{YZ} \end{Bmatrix} = \begin{Bmatrix} \sigma_x \\ \sigma_Y \\ \sigma_Z \\ \tau_{XY} \\ \tau_{XZ} \\ \tau_{YZ} \end{Bmatrix} - \begin{Bmatrix} \alpha P \\ \alpha P \\ \alpha P \\ 0 \\ 0 \\ 0 \end{Bmatrix} = \begin{Bmatrix} \sigma_x \\ \sigma_Y \\ \sigma_Z \\ \tau_{XY} \\ \tau_{XZ} \\ \tau_{YZ} \end{Bmatrix} - \begin{Bmatrix} \alpha(H - Ele)\gamma_w \\ \alpha(H - Ele)\gamma_w \\ \alpha(H - Ele)\gamma_w \\ 0 \\ 0 \\ 0 \end{Bmatrix} \quad (3)$$

Where α is the Biot's coefficient and σ_{ij} is the stress components.

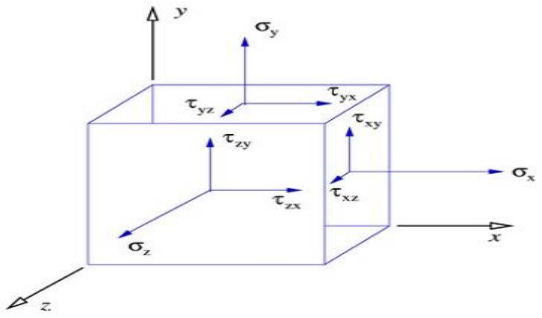

Figure 5 - Stress components in the three-dimensional model

If the compressibility of isolated soil particles and the porous medium equal C_s and C_m, and the fluid compressibility equals C_f, the Biot's coefficient is calculated from Equation (4). If C_s approximately equals 0, Equation (3) will be the same Terzaghi equation.

$$\alpha = 1 - \frac{C_s}{C_m} \quad (4)$$

On the other hand, the relation between stresses and strains are established by the Hooke's law, as consisted with Equation (5).

$$\begin{aligned} \sigma'_{xx} &= -\left(K + \frac{4}{3}G\right)\varepsilon_{xx} - \left(K - \frac{2}{3}G\right)\varepsilon_{yy} - \left(K - \frac{2}{3}G\right)\varepsilon_{zz} \\ \sigma'_{yy} &= -\left(K + \tfrac{4}{3}G\right)\varepsilon_{yy} - \left(K - \tfrac{2}{3}G\right)\varepsilon_{xx} - \left(K - \tfrac{2}{3}G\right)\varepsilon_{zz} \\ \sigma'_{zz} &= -\left(K + \frac{4}{3}G\right)\varepsilon_{zz} - \left(K - \frac{2}{3}G\right)\varepsilon_{xx} - \left(K - \frac{2}{3}G\right)\varepsilon_{yy} \end{aligned} \quad (5)$$

Assuming Equation (6) is also established:

$$\sigma'_{xy} = \sigma'_{yx} = 2G\varepsilon_{xy} \text{ and } \sigma'_{xz} = \sigma'_{zx} = 2G\varepsilon_{xz} \text{ and } \sigma'_{yz} = \sigma'_{zy} = 2G\varepsilon_{yz} \quad (6)$$

Where, ε_{xx} is the strain components, K is the Young's modulus and G is the shear modulus.

$$K = \frac{1}{C_m} \quad (7)$$

$$G = \frac{3K(1-2\mu)}{2(1+\mu)} \quad (8)$$

Consistent with Equation (5), the changing of the effective stress causes the porous medium to deform. In other words, as the effective stress increases, the porous medium gets compacted and causes subsidence. The increased effective stress and soil compression may occur by three mechanisms in the aquifer: increasing the total stress level, reducing pore-water pressure and combination of the two previous mechanisms. In the free aquifer, as the groundwater level goes down, as consistent with Equation (9), effective stress increases which causes the porous medium to subside. In closed aquifer, there is also a similar mechanism which, again, the same equation can be used to calculate the reduced pore-water pressure, followed by increased effective stress.

$$\Delta\sigma'_A = -\Delta p_A = \gamma_w \Delta H \quad (9)$$

Now, considering the Biot's balance equation, as consistent with Equation (10), and applying finite element method to a linear equation system, we'll conclude that this equation system is solved by iterative methods of solving linear equation on COMSOL software, which yields the total deformation and hydraulic head for each time interval.

$$\alpha \frac{\partial \varepsilon}{\partial t} + S\gamma_w \frac{\partial H}{\partial t} - \frac{\partial}{\partial x}\left(k_x \frac{\partial H}{\partial x}\right) - \frac{\partial}{\partial y}\left(k_y \frac{\partial H}{\partial y}\right) - \frac{\partial}{\partial z}\left(k_z \frac{\partial H}{\partial z}\right) = 0 \quad (10)$$

Where S indicates the coefficient of storage, calculated from Equation (11). Here, n is the formation porosity, k_i is the hydraulic conductivity of the formation in different directions and H is the total hydraulic head.

$$S = nC_f + (\alpha - n)C_s \quad (11)$$

By applying the finite element method approximation to the Biot's equation, Equation (12) is achieved:

$$\begin{bmatrix} [A] & [B] & [C] & [D] \\ [E] & [F] & [G] & [H] \\ [I] & [J] & [L] & [M] \\ [N] & [O] & [P] & [Q] + \Delta t[R] \end{bmatrix} \begin{pmatrix} \{u_1\} \\ \{v_1\} \\ \{w_1\} \\ \{H_1\} \end{pmatrix} = \begin{pmatrix} \{F_{x1}\} + [D]\{H_{\text{ini}}\} \\ \{F_{y1}\} + [G]\{H_{ini}\} \\ \{F_{z1}\} + [I]\{H_{ini}\} \\ \{QQ\} \end{pmatrix} \quad (12)$$

Where vectors u_1, v_1 and w_1, are levels of displacement in x, y and z directions. F is the force applied to the element and H is the hydraulic head at the beginning of the modeling process, while Δt shows the time-steps of the solution.

Equation (12) can be solved by using various numerical methods and applying the boundary conditions on groundwater flows. Out of the different methods, the finite element method is more proportionate to the current research, because it is more flexible compared to the finite difference method. Thus, the COMSOL software, which works on the finite element method, is used [5].

3.2.2. Implementing the Model

To implement the model, geological, geo-mechanical and hydrological data of the area under study were entered into software. The area has six separate subsurface units including three units of aquifers and three units of fine-grained clay layers with low hydraulic conductivity. The clay layers thickness varies in the scope of the study. These six separate layers have been derived from geology map data from the Geological Survey and Mineral Exploration of Iran, and from geo-mechanical parameters of the layers as given in Table 1 [26].

Table 1- Geo-mechanical characteristics of geological layers

Model layers	Density Kg/m^3	Young's modulus Gpa	Bulk modulus Gpa	Poisson's ratio	Porosity	Horizontal hydraulic conductivity (m/s)	Horizontal hydraulic conductivity (m/s)
First fine-grained clay	16.55	0.41	0.42	0.35	0.1	5.10*10-10	3.40*10-10
First aquifer	16.45	0.35	0.32	0.34	0.5	4.83*10-6	3.86*10-6
Second fine-grained clay	16.88	0.83	1.27	0.34	0.8	3.30*10-10	2.20*10-10
Second aquifer	19.87	3.36	4.63	0.34	0.5	1.17*10-5	9.36*10-69
Third fine-grained clay	20.51	4.37	9.14	0.41	0.9	2.09*10-10	1.40*10-10
Third aquifer	21.76	9.1	10.18	0.38	0.5	2.61*10-5	2.08*10-5

Also, consistent with Figure (6a), surface topography and layering were produced in the COMSOL software; in the end, consistent with Figure (6b), discretization was performed to solve the equations governing the geometry intended in the software. The total number of three-dimensional elements amounted to 175258 elements following discretization of the model's geometry. The model's enlargement level in the direction perpendicular to the layers (z) was shown to be 20 times larger.

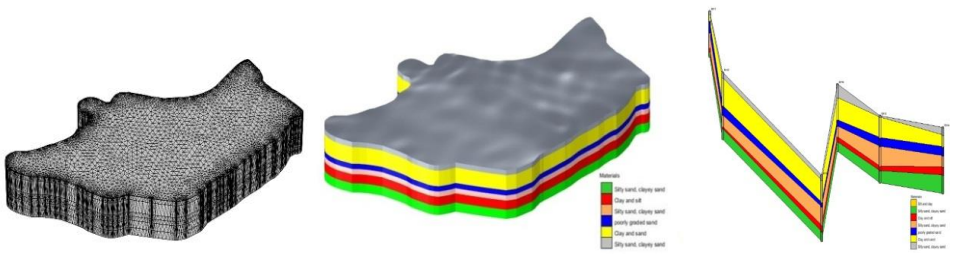

(b) (a)

Figure 6-a) Geological and topographic model b) Three-dimensional discretization model

As regards the boundary conditions of the problem, first, readings of the hydraulic heads were prepared by installed piezometers since the beginning of the simulation in 2003, and then entered into the software. The number of the wells and their depletion levels were entered into the COMSOL using the Well Condition. Considering the multi-physical nature of the problem of subsidence, the model's mechanical boundary conditions had to be met. For this, the model's bottom was defined as the bedrock in the model which was bound by the level of the zero-displacement rate, as the upper surface of the model was defined as a free surface that could be displaced in all directions. Lateral boundaries of the model were simply free in the vertical direction of displacement, but were bound in the horizontal direction of displacement.

3.2.3. Verification

For validation, the root-mean-square error (RMSE) method, as shown in Relation (13), and efficiency factor, as shown in Relation (14), were used using levelling and computational data for 8 critical and non-critical points of the model from 2001 to 2016, later analyzed. According to Table 2, the RMSE approaches zero, while the efficiency factor is larger than 0.5, tending to one. It can be said that the executed model enjoys good validation [40].

$$\mathrm{RMSE} = \frac{\sqrt[2]{\sum_{i=1}^{n} \langle Xobsi - Xmodeli \rangle 2}}{\sqrt[2]{n}} \quad (13)$$

$$E = 1 - \frac{\sum_{i=1}^{n} \langle Xobsi - Xmodeli \rangle 2}{\sum_{i=1}^{n} \langle Xobsi - Xobs \rangle 2} \quad (14)$$

Where $X_{Obs.i}$ is the observed value at time or place i, $X_{model.i}$ is the calculated value at time or place $_i$ and xobs is the mean observed value.

Table 2: The square of the mean squares of the error and the efficiency coefficient of the selected points 2002, 2011 and 2016

Location	Name	X(m)	Y(m)	RMSE			Efficiency coefficient		
				2006	2011	2016	2006	2011	2016
P3	Ahmad Abad Jan Separ	5131100	3934910	0.1294	0.0923	0.0845	0.9665	0.8696	0.9792
P4	Ahmad Abad Mostofi	518996	3943371	0.0258	0.0746	0.0713	0.9996	0.9835	0.8662
P5	Eskman	510900	3939980	0.0509	0.1061	0.0229	0.9993	0.9988	0.9441
P7	Balaban	510460	3943700	0.1043	0.0580	0.1821	0.9556	0.9984	0.9517
P10	Pelain	536265	3938078	0.0417	0.0824	0.1570	0.9613	0.9498	0.9111
P11	Jafarabad Jangal	528264	3936008	0.286	0.272	0.211	0.9988	0.9978	0.8813
P18	Shahed Shahr	508416	3936834	0.0601	0.1464	0.0753	0.9985	0.9964	0.9987
P19	Shams Abad	525068	3942697	0.0322	0.0042	0.368	0.9985	0.9999	0.9990

The common method to provide calibration results of the model is the scatter diagram of data [26]. Figure 7 shows the outputs of the software from 2003 to 2019 in 24 selected points (consistent with the place oof piezometers) as well as annual levelling withdrawals of their corresponding points. Thus, the coefficient of determination is 0.97 (R^2=0.97), indicating higher consistency and correlation between data from the software and levelling data.

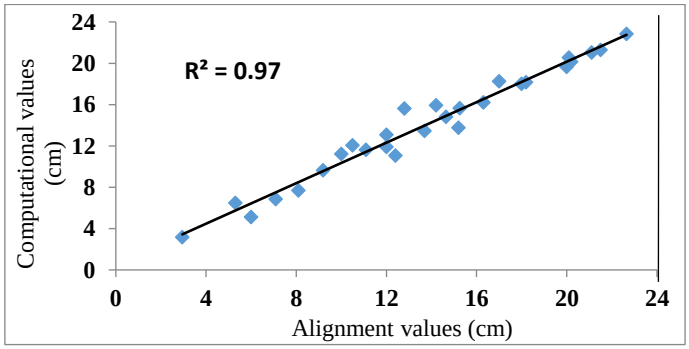

Figure 7- Fitting diagram of observed values based on calculated subsidence values

Again, for validation, the Sentinel 1 radar interferometry images of the area under study for 2013 to 2016 were prepared, as shown in Figure 8 [30].

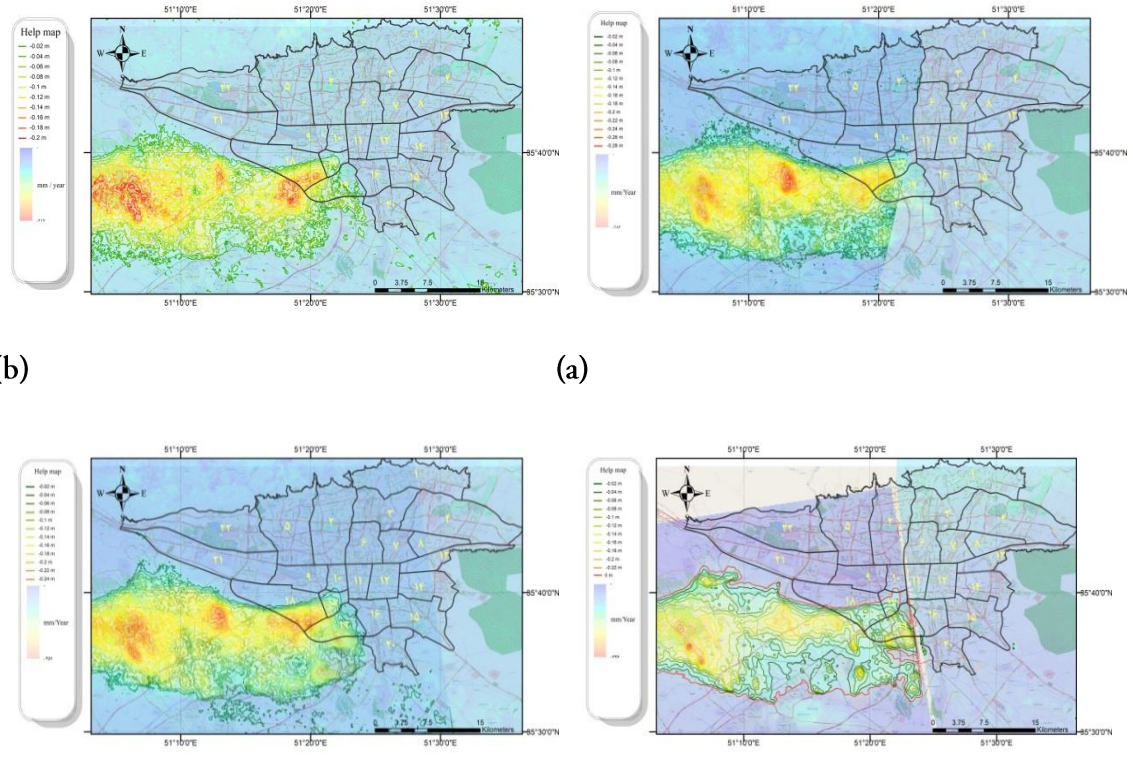

Figure 8- Contour maps of land subsidence using Sentinel 1 radar interferometry images in study area in a)2003, b)2006, c)2010 and d)2016

Comparing the radar interferometry images and their corresponding cosubsidence maps revealed that the COMSOL software output, seen in Figure 9 in the form of co-subsidence curves, enjoys an acceptable match between the images and the maps in terms of subsidence zone.

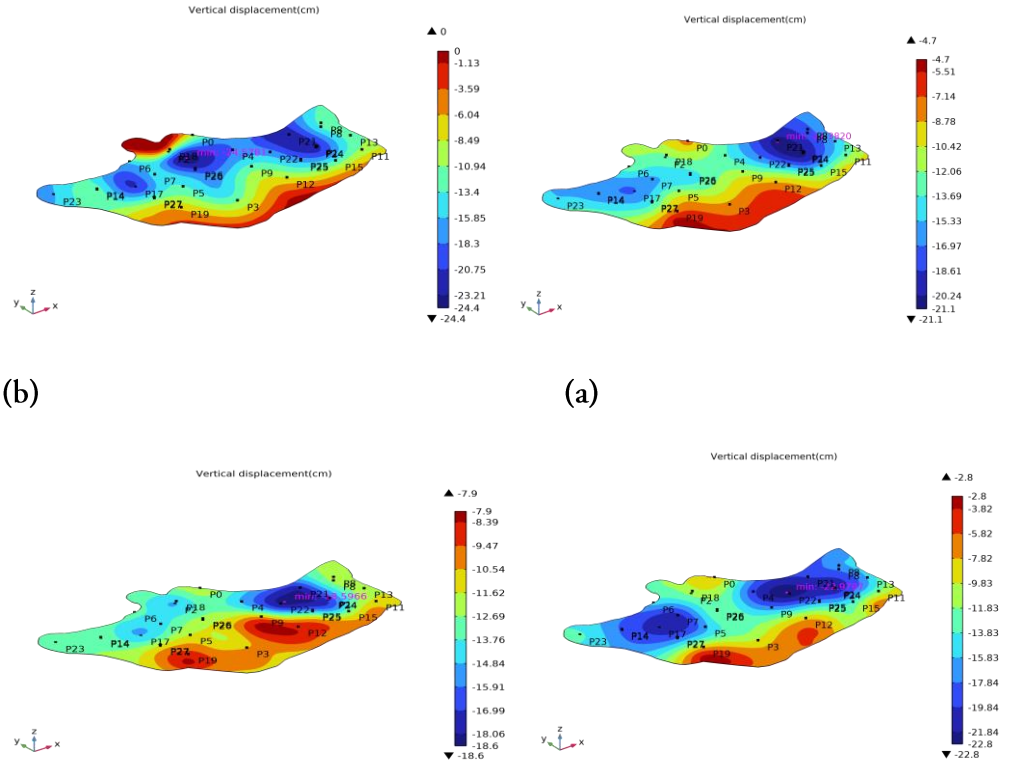

(b) (a)

(d) (c)

Figure 9 – Contour maps of land subsidence in study area in a) 2003, b)2006, c)2010 and d)2016

Later, for further verification of the model, the groundwater level curve is simulated in two states, as shown by Figure 10, and the measurements by installed piezometers from 2015 to 2016 are compared which noted no significant difference.

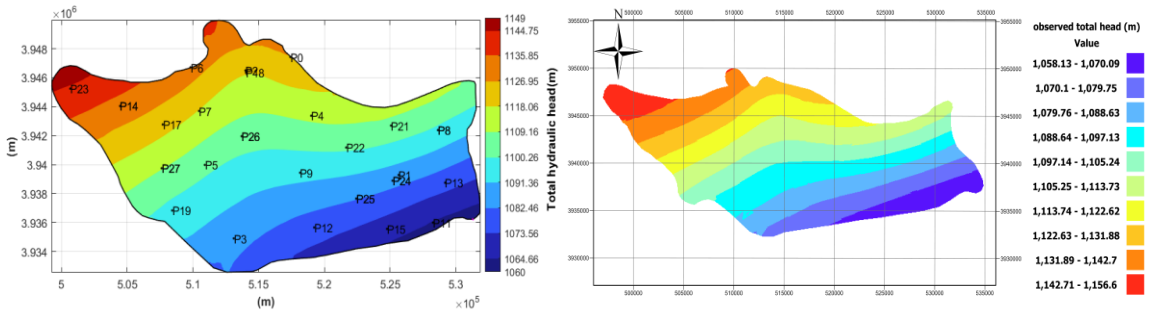

(b) (a)

Figure 10- Total hydraulic head a) observation b) calculated from 2015 to 2016

Also, in order to check and show the more detailed agreement of observational and model calculation data, according to Figure 11, the hydrograph of the underground water unit of two points of Ahmedabamustafi and Eskman during the years 2003-2019 were compared with each other, and no significant difference was observed.

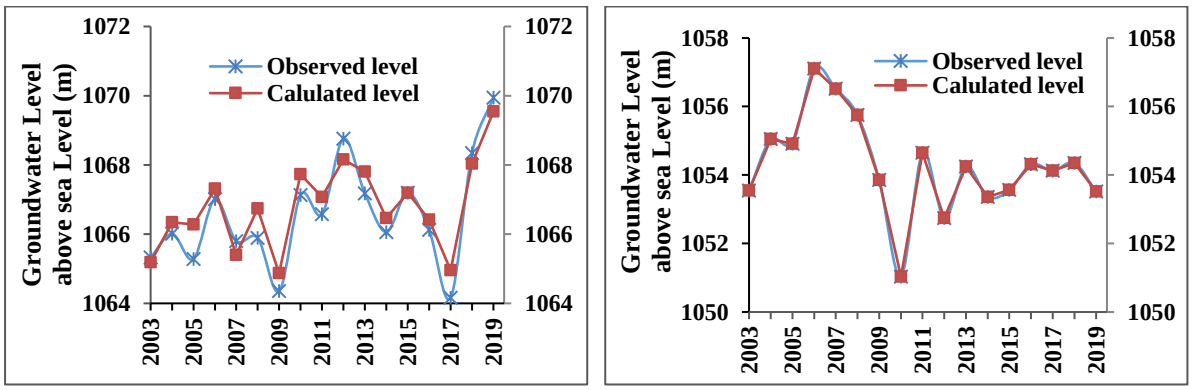

(b) (a)

Figure 11- Observatory and computational hydrograph of groundwater unit in a) Ahmadabad Mostofi b) Eskman

4. Results

After entering the geological data of the layers, hydrology and annual pumping rate, the selection of the hydraulic conditions and application of boundary conditions of the model were implemented. Later, the following findings were provided after selecting the year of starting the modeling and time-step as well as the ending year.

4.1. Estimation of subsidence in 2031

As suggested by verification results, there is a good match between actual and computational data; therefore, with great confidence, subsidence in future years can be estimated by the COMSOL software. Figure 12 has projected the phenomenon of subsidence until 2031 by using the software, assuming the continuation of the current conditions of the aquifer's level changes. The results indicated that the average subsidence of the area under study will be around 13.19 cm during the year 2031, and 17.15 and 18.38 cm in critical points of the plain such as Goldasteh and Balaban, respectively.

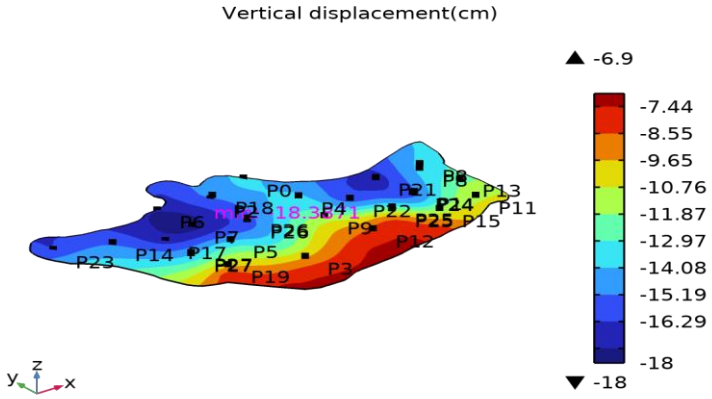

Figure 12- Contour map of land subsidence in study area in 2031

4.2. Analyzing the subsidence using effective parameters

Research results suggested that such parameters as clay thickness, aquifer level changes and number of geological units are involved in land subsidence. Later, each of these parameters are analyzed.

4.3. Analyzing the relationship between subsidence and aquifer's level changes

One of the main factors contributing to land subsidence is changes occurring to groundwater resources, demonstrated by changes of the aquifer levels. To analyze the relationship between subsidence and this parameter, several critical and non-critical points of the plain under study were examined in terms of subsidence rates. Ahmad Abad and Balaban were selected as critical points and Jafar Abad and Eskman as non-critical points. The relationship between cumulative subsidence and aquifer level changes in areas intended is illustrated in diagrams of Figure 12. As shown by the diagrams, the cumulative subsidence rate experiences an increasing trend of various rates. Meanwhile, some points of the aquifer level have had a general downward trend, but some others had a general upward trend. However, the total aquifer level has seen a downward trend, as consistent with hydrograph 3.

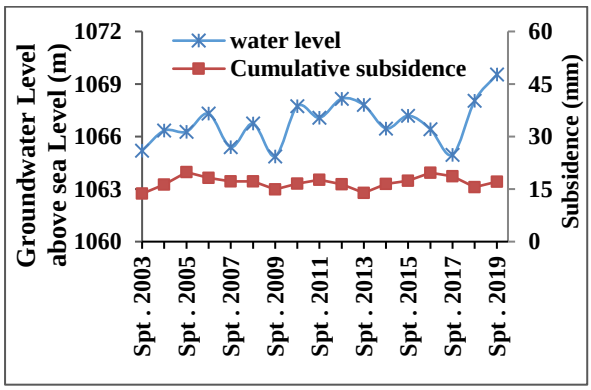

) a)

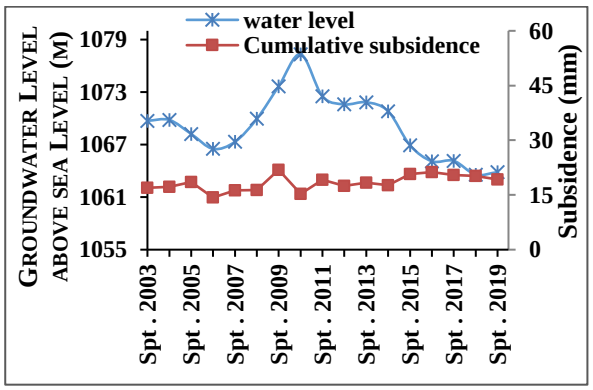

(b(

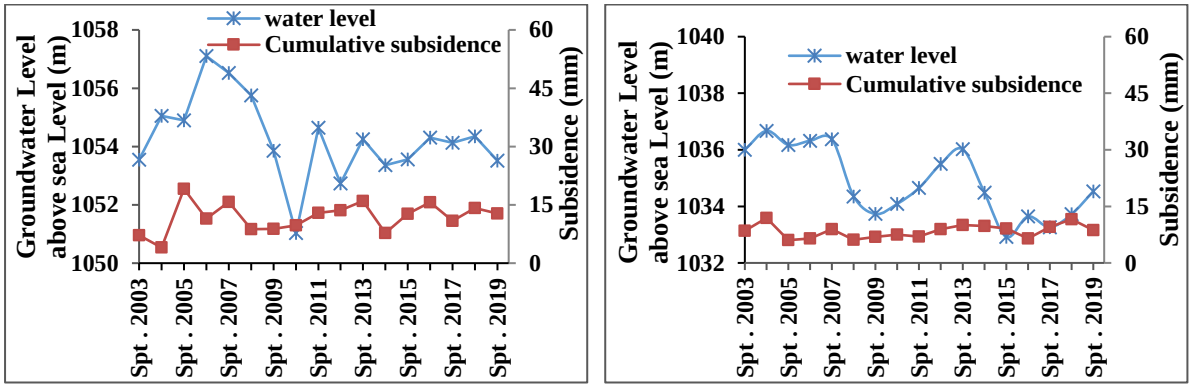

) c ( ) d(

Figure 13 - Diagrams of the relationship between cumulative subsidence from 2003 to 2019 with changes in aquifer levels in points, a) Balaban, b) Ahmadabad Mostofi, c) Jafarabad Jangal, and, d) Eskman

For a more accurate analysis of the relationship between subsidence and aquifer level changes, diagrams in Figure 14 are illustrated. An analysis of these diagrams is as follows:

- The aquifer level changes reveal their impacts on subsidence with a time delay of 1 to 3 years, with the 2-year time delay having the highest frequency. In Ahmad Abad, for example, an increase in the water level in 2009 reduced the subsidence rate in 2011, or in Balaban, an increase in the rate of subsidence, caused by reduced water levels in 2010, was noted three years later in 2013. Also, an increase in the rate of subsidence in Jafar Abad in 2016, which was caused by reduced water levels, was noted two years earlier in 2014.

- As the aquifer level changes increased, the rate of subsidence experienced a higher rate and a lower time delay. As shown by the diagrams, a 4-cm reduction of the aquifer levels from 2009 to 2010 in Eskman caused subsidence at a greater rate of changes from 2010 to 2013, with the annual subsidence rate of this area increasing to 16 cm from 10 cm in this time period. Meanwhile, smaller aquifer level changes in Jafara Abad Jangal (around 1 m) caused subsidence of 1.5 cm, as noted from 2008 to 2011.

- The lower aquifer level changes, i.e., water level changes occur at longer periods of time, the rate of land subsidence will be smaller, and vice versa, as the changes occurring in shorter periods of time, the resulting subsidence, noted with time delay, will be greater in scales. This is more noticeable in comparison to diagrams of Balaban where aquifer level changes occur at longer periods of time, and in Ahmad Abad Mostofi where the changes occur at shorter periods of time. As seen, in Balaban, water level has dropped by 12 m from 2010 to 2016; but the subsidence diagram that begins from 2013 reveals a milder rate of subsidence with changes of less than 5 cm. In other words, for every 1 m of water level drop, subsidence will increase by 0.4 cm. In Ahmad Abad Mostofi, however, the situation is reverse, i.e., since 2006 onwards when water levels experienced alternative down- and upward trends, albeit milder, of maximum over 3 cm each year,

the corresponding subsidence change rates of 2009 onwards have been experiencing changes greater than 6 cm, i.e., for every 1 m of water level drop, 2 cm of subsidence has occurred. As seen, this rate is 4 times as many in Balaban.

- The steep slope of subsidence in early years is due to the emptying of a large volume of water inside the voids and inter-granular voids as well as the fast compaction of the upper layers of the aquifer. Considering the aquifer's level and depth decreases, and hydraulic bonding between the layers, there are fewer voids and pores compared to early years, causing subsidence of slower rate compared to early years.

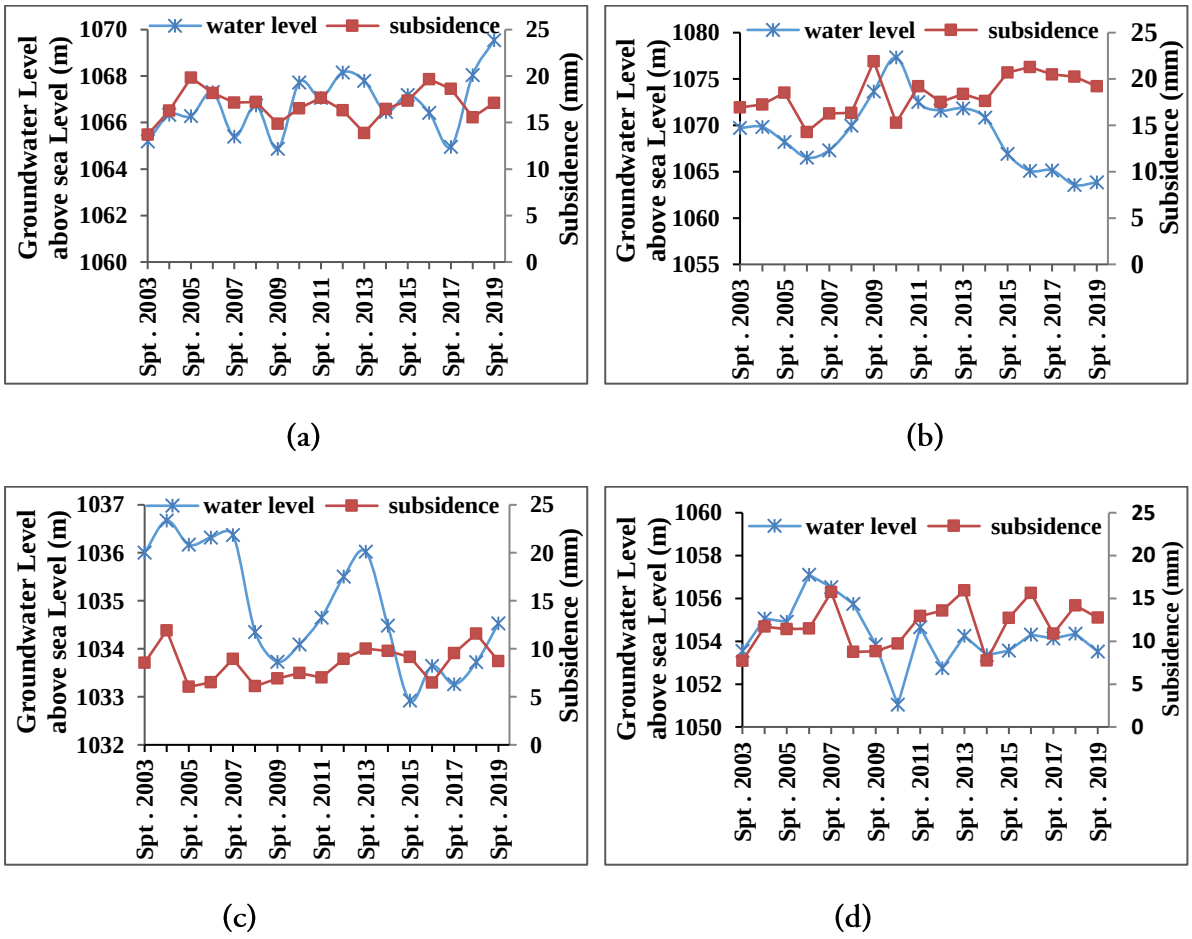

Figure 14- Composite diagrams of subsidence and hydrography a) Balaban, b) Ahmadabad Mostofi, c) Eskman, and, d) Jafarabad Jangal

4.4. Analyzing the relationship between subsidence and number of geological units and earth's type

The area under study in the Tehran-Shahriar plain involves six isolated subsurface units, including three units of aquifers and three units of compressible fine-grained clay layers of low permeability. As Figure (6a) shows, the area has a multi-layer aquifer system.

The different type of soil layers has a significant role in layer deformation which is due to the uncontrolled groundwater abstraction that subsequently causes subsidence. The presence of fine-grained sediments such as clay and silt does not allow for the feeding and permeation of water into the aquifer. Following uncontrolled abstraction of groundwater, fine grains will become irreversibly consolidated and cause land subsidence; on the other hand, coarse-grained sediments like sand and gravels have much smaller impact on the incidence of subsidence compared to the fine-grained sediments, which is due to their higher permeability.

The thickness of soil layer is also another effective parameter that is directly related with the subsidence of each region, which, if the thickness of the fine-graine layer increases, it is more likely to experience subsidence.

Therefore, different subsidence rates or relevant time delays in some areas, as compared to other areas, are due to the aquifer levels caused by geological characteristics of the region including soil type and thickness.

The said rates are more notable in Pelain, Ahmad Abad Jan Separ, Shams Abad and Shahed Shahr. In all these regions, subsidence follows an almost fixed general trend but with different hydrographs. Figure 15 shows that water level in Pelain is decreasing, while it is increasing in Ahmad Abad, Shams Abad and Shahed Shar.

Subsidence in Shamsabad is very high, while it is at its lows in Shahed Shahr. This is due to the similarity of the subsidence trend in selected areas with different hydrographs, as well as heterogeneity of the land type in these regions. According to the geological map of the area under study [29], there is a sand and clay layer with high thickness and high percentage of sand in Pelain which, despite reducing water levels fail to cause a significant increase in the land subsidence rate. As well, there is a sand and clay layer with high thickness and high percentage of clay in Shams Abad which, unlike Pelain, the increase in the water level does not reduce land subsidence.

The presence of thick coarse-grained sand layer in Shahed Shahr and Ahmad Abad Jan Separ does not cause the subsidence to decrease as the aquifer water level increases. In this region, subsidence has a low rate, also.

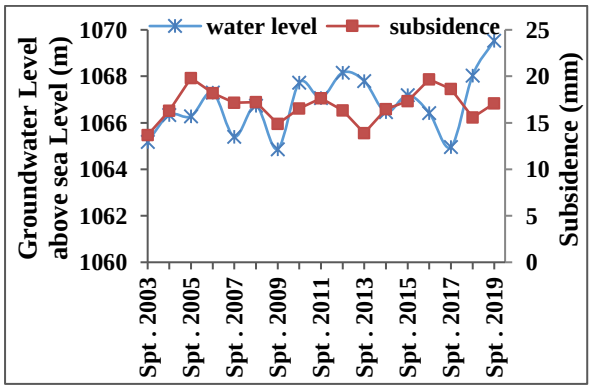

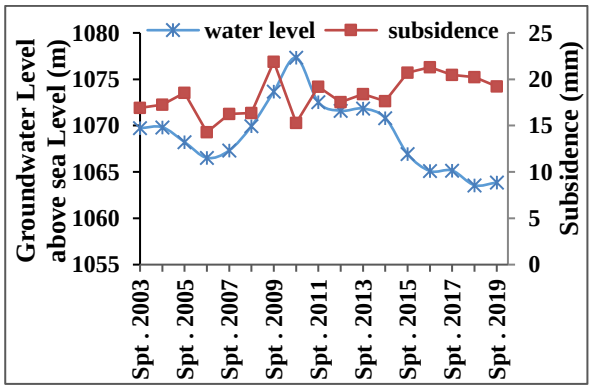

) a ( ) b(

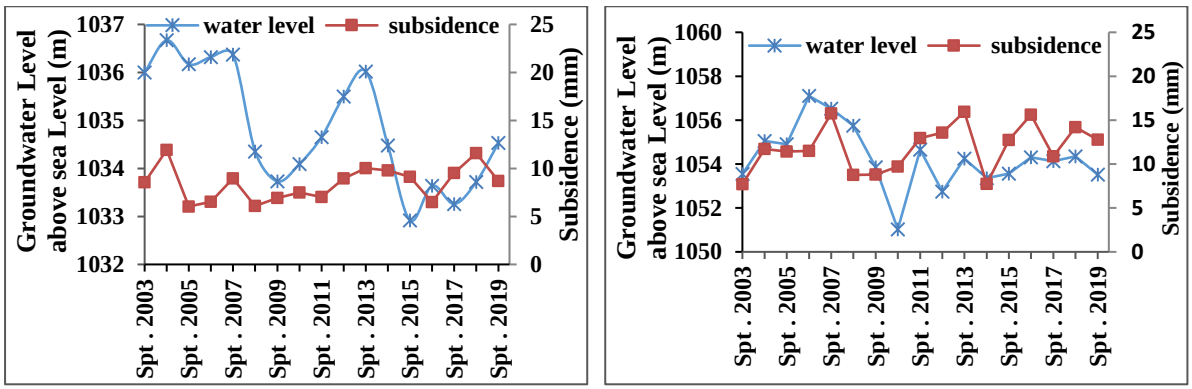

) c ( ) d(

Figure 15- Combined subsidence diagram and hydrograph of points a) Balaban, b) Ahmadabad Mostofi, c) Eskman, and d) Jafarabad Jangal

5. Conclusion

This study used the COMSOL software to calculate the subsidence in the area under study and investigated the numerical model data from 2003 to 2019 in 24 selected points using levelling acquisitions, Sentinel 1 interferometric images, acquired hydraulic heads and verification computations. The coefficient of determination was 0.97, indicating acceptable correlation between data values, good match between radar interferometric images and subsidence zoning maps based on software outputs, and full similarity between the groundwater level curve in two states of simulated and measured piezometers in the water year of 2015 to 2016; in the meantime, the RMSE values tended to zero, while efficiency coefficients were larger than 0.5 and tended to 1. Then, the average subsidence rate in the area was estimated to amount to 13.19 cm by 2031, and to 18.38 cm in critical points. Then, findings suggested that the maximum subsidence caused by groundwater drop in early years was noted to attain higher rates in upper layers of the aquifer; over time, the rate of subsidence was gradually noted to have a slower pace in the upper layers of the aquifer level and over the earth's surface, following the filling of the soil particle voids and considering the hydraulic connection between the layers.

Also, the parameters affecting the subsidence and relevant changes were examined. The most important parameters included changes to the aquifer levels due to increased agriculture territories, density of authorized and unauthorized agriculture wells of high discharge rates, pr-existing geological structures in the region and radical changes of bedrock height levels. Also, groundwater level changes in the time interval were more factors that contributed to the subsidence rate and patterns.

The effects of changing aquifer levels of the subsidence are noted with a time delay of 1-3 years, as the average 2-year delay has the highest frequency. Also, with the increasing changing levels, the

subsidence rate is noted with a greater rate and less time delay. The less frequent aquifer table changes, i.e., water level changes occurring over a longer period, the less the ground subsidence. Other parameters affecting this region's subsidence are the ground type and the number of geological units. The presence of fine-grained and clay layers, especially with higher thickness, could be an effective factor in the ground type and parameter. The overall result suggests that aquifer level changes are more directly related to subsidence changes in this region.

References

1- Bajni, G., Apuani, T., Beretta, G.P., 2019. Hydro-geotechnical modelling of subsidence in the Como urban area. Eng. Geol. 257, 105144.
2- Biot M. General solutions of the equations of elasticity and consolidation for a porous material. J Appl Mech 1956:23(1):91-6.
3- Bot MA.Theory of elasticity and consolidation for a porous anisotropic solid J Appl Phys 1955 ; 26(2): 182-5.
4- Biot MA. Mechanics of deformation and acoustic propagation in porous media. J Appl Phys 1962;33(4): 1482-98.
5- Biot, M.A., 1941. General theory of three-dimensional consolidation. J. Appl. Phys.12 (2):155–64.
6- Comsol Multiphysics, Software Guide Version 5.1.
7- Castellazzi, P., Garfias, J., Martel, R., Brouard,C.,Rivera.A.,2017. InSAR to support sustainable urbanization over compacting aquifers: the case of Toluca Valley, Mexico. Int. J. Appl. Earth Observ. Geoinf. 63, 33–44.
8- Conway, B.D., 2016. Land subsidence and earth fissures in south-central and southern Arizona, USA. Hydrogeol. J. 24(3), 649–655.
9- Ding, P., Jia, C., Di, S., Wang, L., Bian, C., Yang, X., 2020. Analysis and prediction of land subsidence along significant linear engineering. Bull. Eng. Geol. Env. 79(10), 5125–5139.
10- Duc-Huy Tran, Shih-Jung Wang, Quoc Cuong Nguyen.,2022, Uncertainty of heterogeneous hydrogeological models in groundwater flow and land subsidence simulations–A case study in Huwei Town, Taiwan,Engineering Geology,Volume 298.
11- Figueroa-Miranda, S., Tuxpan-Vargas, J., Alfredo Ramos-Leal, J., Manuel Hernandez-Madrigal, V., Irene Villasenor-Reyes,C.,2018.Land subsidence by groundwater over-exploitation from aquifers in tectonic valleys of Central Mexico: a review. Eng. Geol. 246, 91–106.
12- Gambolati, G, Gatto, P, Freeze, R.A.,1974,2005. Mathematical simulation of the subsidence of Venice. Results: American Geophysical Union, Water Resources Research, 10(3): 563–577.
13- Geological Survey of Iran., 2005, study of land subsidence in Tehran-Shahriar plain, Tehran.

14- Gong, X., Geng, J., Sun, Q., Gu, C., Zhang, W., 2020. Experimental study on pumping-induced land subsidence and earth fissures: a case study in the Su-Xi-Chang region, China. Bull. Eng. Geol. Environ. 79(9), 4515–4525.

15- Guzy, A., Malinowska, A., 2020. State of the art and recent advancements in the modelling of land subsidence induced by groundwater withdrawal. Water 12(7), 2051.

16- Chao-Feng Zeng, Shuo Wang, Xiu-Li Xue, Gang Zheng, Guo-Xiong Mei., 2021, Evolution of deep ground settlement subject to groundwater drawdown during dewatering in a multi-layered aquifer-aquitard system: Insights from numerical modelling,Journal of Hydrology,Volume 603, Part C.

17- Herrera-Garcı´a, G., Ezquerro, P., Toma´s, R., Be´jar-Pizarro, M., Lo´pez-Vinielles, J., Rossi, M., et al., 2021.Mapping the global threat of land subsidence. Science (American Association for the Advancement of Science). 371(6524), 34–36.

18- Hsieh, P.A., 1996. Deformation-induced changes in hydraulic head during ground-water withdrawal. Ground Water (34) 6: 1082-1089.

19- Hu, R.L., Yue, Z.Q., Wang, L.C., & Wang, S.J.,2004. Review on current Status and challenging issues of and subsidence in China. Engineering Geology, 76:6577.

20- H.Guo,(2015) , Groundwater- abstraction induced land subsidence and groundwater regulation in the North China Plain, piahs- 372.

21- Janbaz Fotmi, M, et al., 2020, Investigation of land subsidence due to changes in groundwater water level using radar differential interferometry method: A case study of Qazvin province, Journal of Water Resources Research,16(3):147-133.

22- Jia, C., Zhang, Y., Han, J., Xu, X., 2017. Susceptibility area regionalization of land subsidence based on extenics theory. Clust. Comput. 20, 53–66.

23- LoW., Purnomo S. N., Dewanto B. G., Sarah D., Sumiyanto., 2022. Integration of numerical models and InSAR techniques to assess land subsidence due to excessive groundwater abstraction in the coastal and lowland regions of Semarang City. Water (Basel) 14(2), 201.

24- Lee, S.& park, I., 2013. Application of decision tree model for the SBAS-DINSAR technique to fault creep: A case 15-15-Lashkaripour, G, Ghafouri, M, Rostami Barani, H., 2020, Investigation of the causes of fissure formation and subsidence in the west of Kashmar plain, Geological Studies, 1(1):111-95.

25- Mahmoudpour, M., Khamehchiyan, M., Nikoudel, M.R., Ghassemi, M.R.,2013, Characterization of regional land subsidence induced by groundwater withdrawals in Tehran, Iran, JGeope 3(2): 49-62.

26- Mahmoudpour, M., 2015, The role of interaction of engineering geological features and groundwater abstraction in the mechanism and pattern of land subsidence in the southwest of Tehran, PhD thesis in Engineering Geology, Tarbiat Modares University, Tehran.

27- Mohammad Khan, S, Ganjian, H, Grossi , L, Zanganeh Tabar, Z., 2020, Evaluation of the effect of groundwater depletion on subsidence using radar images, study area, Qorveh plain, Geographical Data Quarterly 112(28) : 229-220.

28- Nadiri, A, Taheri, Z , Barzegari, G, Dedeban, K., 2018, Providing a framework for estimating aquifer subsidence potential using genetic algorithm, Journal of Water Resources Research, 4(2):185-174.

29- Nadiri, A, Monafi Azar, A, Khamehchian, M., 2018, Comparison of aquifer subsidence vulnerability in southwestern Tehran plain with simple weighting model and genetic algorithm, Journal of Kharazmi Earth Sciences, 4(2): 212-199.[In Persian]

30- Rajabi Khamseh, k, Nikbakht Shahbazi, A, Fatahhayan, H, Zahrabi, N., 2021,modeling of Izeh plain subsidence using MODFLOW mathematical code, Journal of Water Resources Research iran, 16(4): 112-126.

31- Rahmati, O., Golkarian, A., Biggs, T., Keesstra, S., Mohammadi, F., Daliakopoulos., 2019. I.N.: Land subsidence hazard modeling: machine learning to identify predictors and the role of human activities. J. Environ. Manag. 236, 466–480.

32- Sharifi Kia, M., 2010, Investigation of the consequences of subsidence phenomenon in residential lands and plains of Iran, Journal of the Iranian Geological Engineering Association, (3): 3 and (4): 43-58.

33- Sharifi Kia, M , Nikta, M., 2011, Measurement and extraction of hazards resulting from subsidence in residential lands of Greater Tehran, the first seminar on spatial analysis of environmental hazards in Tehran, Tarbiat Moallem University.

34- Terzaghi K,(1925), principles of soil mechanics, IV-settlement and consolidation of clay. Engineeing News-Record, 95 (3): 874-878

35- Taheri Tizro, Abdullah., 2008, Groundwater, Razi University Press, second edition.

36- Tehran Regional Water Company., 2020, inventory of the third period of piezometers and wells in operation of Tehran-Shahriar aquifer, Tehran.

37- Tehran Regional Water Company., 2021, Artificial feeding studies through wide open wells in Tehran-Shahriar plain , Tehran.

38- Verruijt A. PoroElasticity: http://geo.Verruijt. net/.2016.

39- Yu Zhao, Chaolin Wang, Jinqiang Yang, Jing Bi.,2021, Coupling model of groundwater and land subsidence and simulation of emergency water supply in Ningbo urban Area, China,Journal of Hydrology,Volume 594.

40- Zhang, Q.L., Ghen, Y.X., Jilani, G., Shamsi, IH., Yu, Q.G., 2010. Model AVSWAT apropos of simulating non-point source pollution in Taihu Lake basin. Journal of Hazardous Materials 174: 824-830. doi: 10.1016/j.jhazmat.2009.09.127.